Journal of Alloys and Compounds 509 (2011) 6388–6394

Contents lists available at ScienceDirect

Journal of Alloys and Compounds

journal homepage: www.elsevier.com/locate/jallcom

Impedance and electric modulus analysis of Sm-modified $Pb(Zr_{0.55}Ti_{0.45})_{1-x/4}O_3$ ceramics

Rajiv Ranjan[a], Rajiv Kumar[b], Nawnit Kumar[c], Banarji Behera[d], R.N.P. Choudhary[e,*]

[a] Department of Physics, J. Co-operative College, Kolhan University, Jharkhand 831036, India
[b] Department of Physics, J. Worker's College, Kolhan University, Jharkhand 831012, India
[c] Department of Physics and Meteorology, IIT Kharagpur, West Bengal 721302, India
[d] School of Physics, Sambalpur University, Jyoti Vihar, Bula 768019, Orissa, India
[e] Department of Physics, ITER, S.O.A. University, Bhubaneswar 751 013, Orissa, India

ARTICLE INFO

Article history:
Received 18 April 2010
Received in revised form 1 March 2011
Accepted 2 March 2011
Available online 10 March 2011

Keywords:
Ceramics
Sintering
Solid-state reaction
Complex impedance spectroscopy (CIS)

ABSTRACT

The polycrystalline ceramic samples of $Pb_{1-x}Sm_x(Zr_{0.55}Ti_{0.45})_{1-x/4}O_3$ ($x = 0.00$, 0.03, 0.06 and 0.09) were prepared by solid-state reaction technique at high temperature. Electric impedance (Z) and modulus (M) properties of the materials have been investigated within a wide range of temperature and frequency using complex impedance spectroscopy (CIS) technique. The complex impedance analysis has suggested the presence of mostly bulk resistive (grain) contributions in the materials. This bulk resistance is found to decrease with the increase in temperature. It indicates that the PSZT compounds exhibit a typical negative temperature coefficient of resistance (NTCR) behavior. The bulk contribution also exhibits an increasing trend with the increase in Sm^{3+} substitution to PZT. The complex modulus plots have confirmed the presence of grain (bulk) as well as grain boundary contributions in the materials. Both the complex impedance and modulus studies have suggested the presence of non-Debye type of relaxation in the materials.

1. Introduction

The discovery of ferroelectric property in the single crystal Rochelle salt (in 1921) and in the polycrystalline $BaTiO_3$ (in 1940) has created a great revolution in the field of ferroelectricity. It resulted in the development of a wide range of new complex ferroelectric compounds useful for commercial applications and research. Among these compositions, materials based on barium titanate ($BaTiO_3$) and lead zirconate titanate [$Pb(Zr,Ti)O_3$] have been dominated.

Lead zirconate titanate (popularly known as PZT) ceramics [1,2] is the solid-solution of non-centrosymmetric complex system of ferroelectric $PbTiO_3$ (PT; $T_c = 490\,^\circ C$) and antiferroelectric $PbZrO_3$ (PZ; $T_c = 230\,^\circ C$). It has perovskite ABO_3 structure (A = mono or divalent, B = tri-hexavalent ions) in which A-site is occupied by Pb^{2+} ions and B-site by Zr^{4+} or/and Ti^{4+} ions [3–5]. It is the material of great technological importance exhibiting a wide range of piezoelectric, pyroelectric and ferroelectric device applications in the form of actuators and sensors such as pyroelectric detectors, ultrasonic transducers, hydrophones, IR sensors, electro-optic modulators, computer memory and display, microphone, strain sensor for soil applications, etc. [6–12].

The PZT ceramics exhibit three ferroelectric phases; tetragonal in Ti-rich, rhombohedral in Zr-rich and orthorhombic in small titanium compositions. Above Curie temperature, it exhibits paraelectric phase [13–15]. The boundary line between tetragonal and rhombohedral phases is called morphotropic phase boundary (MPB) at which electrical and electromechanical properties of the materials enhance to a great extent [16]. The physical properties and device parameters of PZT based materials appreciably depend on their compositional fluctuations, particle size, nature of substitution/doping at A or/and B site(s), calcination and sintering temperatures, etc. [17–21]. The higher valence cations like La^{3+}, Sm^{3+}, Nb^{5+} as donor (soft) dopant produces Pb-vacancies to maintain electroneutrality that results in high dielectric constant, high electromechanical properties, etc. Whereas the lower valence cations like K^+, Fe^{3+}, Mg^{2+} as acceptor (hard) dopant produces O-vacancies that results in low dielectric constant, low electromechanical properties, etc. [22,23].

An extensive literature survey of pure and modified PZT ceramics [24–31] reveals that most of the reported works in this field are confined to La-modified PZT. It has shown tremendous applications in the solid-state electronic devices. The rare earth element samarium (Sm^{3+}) also satisfies the basic requirements for its substitution

* Corresponding author. Tel.: +91 674 2350181; fax: +91 674 2351880.
E-mail address: crnpfl@gmail.com (R.N.P. Choudhary).

0925-8388/$ – see front matter © 2011 Elsevier B.V. All rights reserved.
doi:10.1016/j.jallcom.2011.03.003

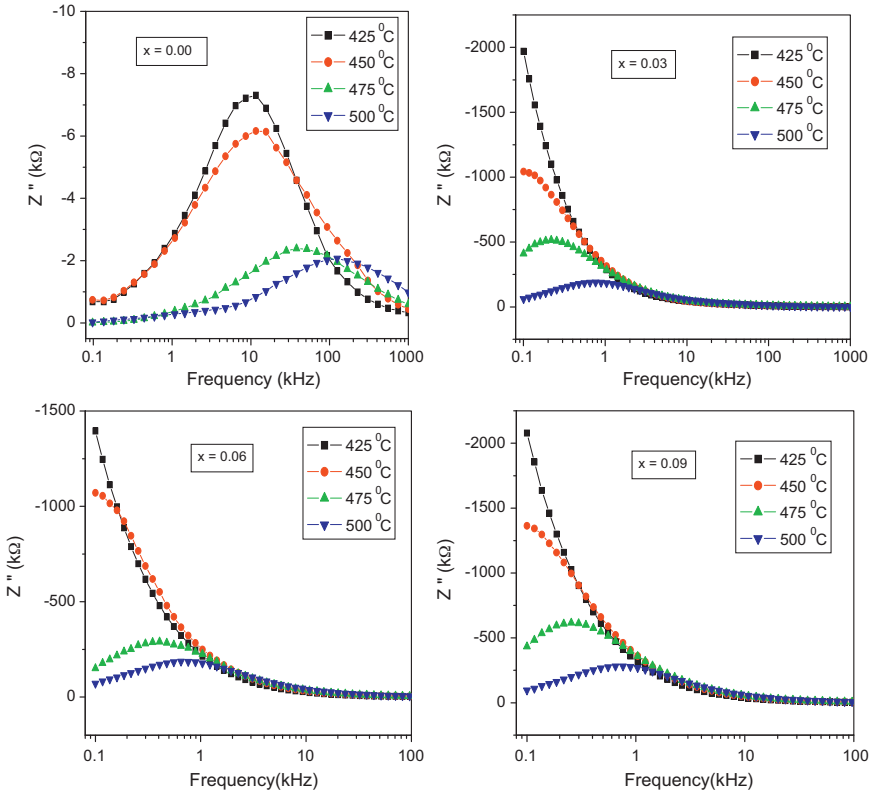

Fig. 1. Frequency–temperature dependence of Z'' of $Pb_{1-x}Sm_x(Zr_{0.55}Ti_{0.45})_{1-x/4}O_3$ with $x = 0.00$, 0.03, 0.06 and 0.09.

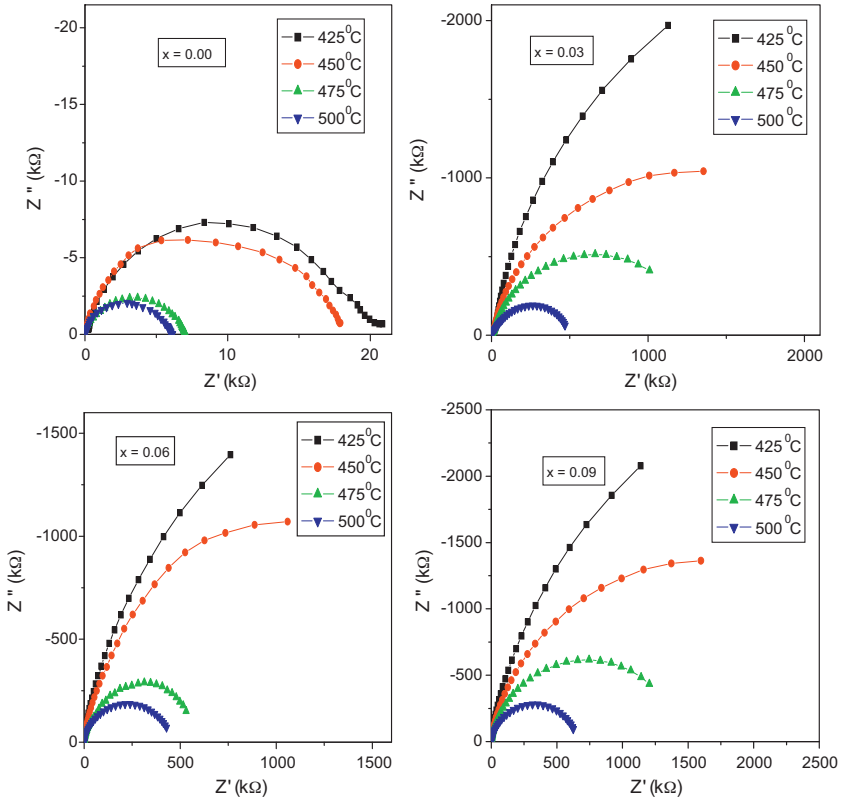

Fig. 2. Variation of Z' with Z'' of $Pb_{1-x}Sm_x(Zr_{0.55}Ti_{0.45})_{1-x/4}O_3$ at selected temperatures with $x = 0.00$, 0.03, 0.06 and 0.09.

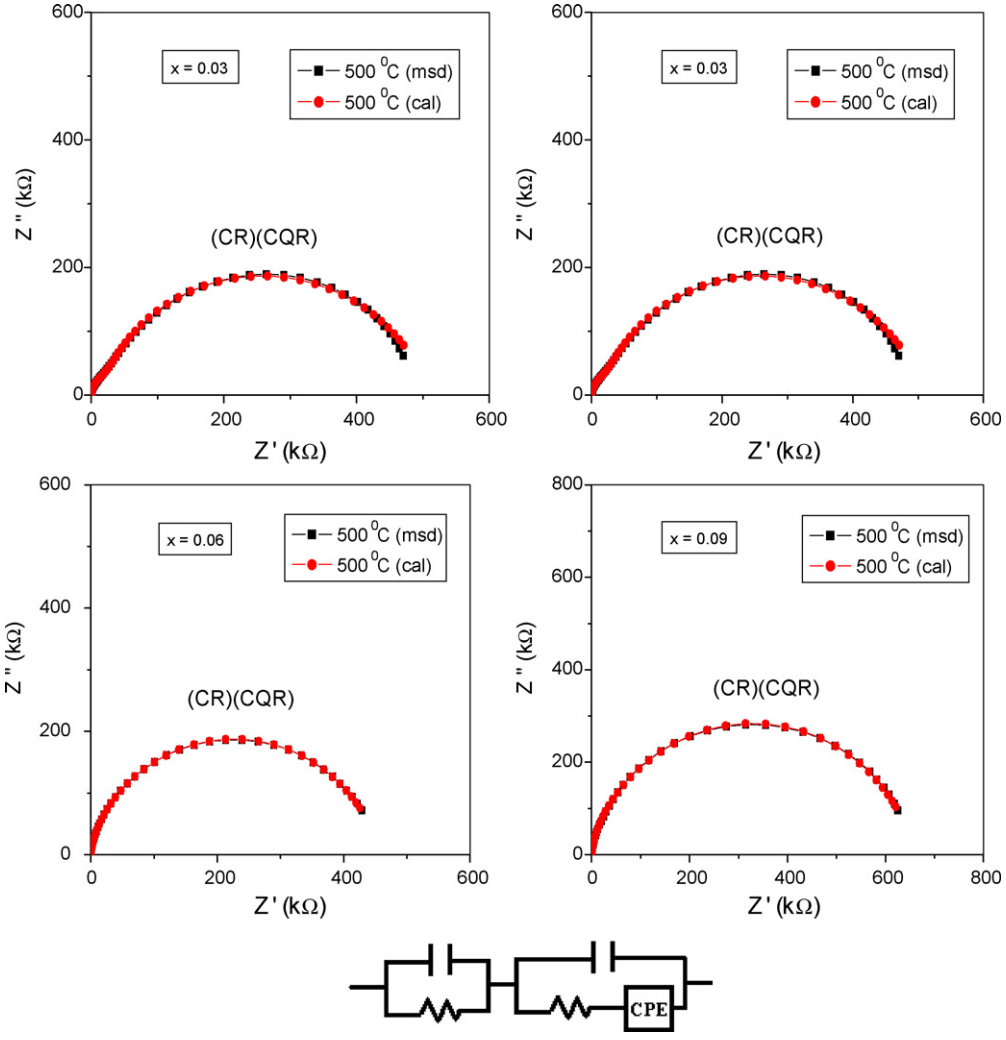

Fig. 3. Comparative fitting of complex impedance plots of $Pb_{1-x}Sm_x(Zr_{0.55}Ti_{0.45})_{1-x/4}O_3$ with $x = 0.00$, 0.03, 0.06 and 0.09 at 500 °C with equivalent circuit.

to PZT [32,33] such as stability of perovskite phase, suitable ionic size (~0.96 Å) to substitute Pb^{2+} (~1.19 Å) at A-site, high Curie-Weiss temperature (~150 °C) usually required by the ferroelectric memory devices, etc. But, only few works have been reported on Sm-modified PZT (called PSZT) ceramics [34–38]. Interestingly, it is found that the PSZT ceramics with Zr/Ti ratio 55/45 exhibits a very high dielectric constant and low tangent loss [39]. But its impedance analysis has not been reported until now though it is close to MPB. In this paper, we report the detailed study of electric impedance and modulus properties of pure and Sm-modified lead zirconate titanate ceramics with Zr/Ti ratio 55/45 using the CIS-technique.

Table 1
Fitting parameters with equivalent circuit [(CR) (CQR)] of PSZT.

Parameters	$x = 0.00$	$x = 0.03$	$x = 0.06$	$x = 0.09$
C [F]	2.345×10^{-9}	2.444×10^{-10}	2.032×10^{-9}	6.259×10^{-10}
R [Ω]	$1.363 \times 10^{+3}$	$1.854 \times 10^{+4}$	$1.238 \times 10^{+5}$	$3.702 \times 10^{+5}$
C [F]	1.205×10^{-10}	1.268×10^{-10}	3.073×10^{-10}	3.011×10^{-10}
A_0	1.907×10^{-7}	2.512×10^{-9}	6.811×10^{-9}	1.834×10^{-8}
n	4.612×10^{-1}	7.5×10^{-1}	6.551×10^{-1}	5.641×10^{-1}
R [Ω]	$4.804 \times 10^{+3}$	$4.936 \times 10^{+5}$	$3.412 \times 10^{+5}$	$3.046 \times 10^{+5}$

2. Experimental details

The PSZT ceramics with chemical composition $Pb_{1-x}Sm_x(Zr_{0.55}Ti_{0.45})_{1-x/4}O_3$ ($x = 0.00$, 0.03, 0.06 and 0.09) were prepared by a simple and inexpensive solid-state reaction technique using the high purity (≥99.9%) ingredients PbO, Sm_2O_3, ZrO_2 and TiO_2 in suitable proportions. 3% of extra lead oxide was added to the mix-

Table 2
The value of bulk resistance (R_b) and grain boundary resistance (R_{gb}) of PSZT.

PSZT with Sm (x)	Temp. (°C)	R_b (Ω)	R_{gb} (Ω)
0.00	425	$1.375 \times 10^{+4}$	$9.678 \times 10^{+3}$
	450	$1.062 \times 10^{+4}$	$9.354 \times 10^{+3}$
	475	$5.523 \times 10^{+3}$	$1.612 \times 10^{+3}$
	500	$4.804 \times 10^{+3}$	$1.363 \times 10^{+3}$
0.03	425	$3.917 \times 10^{+6}$	$2.827 \times 10^{+4}$
	450	$1.835 \times 10^{+6}$	$2.296 \times 10^{+4}$
	475	$1.013 \times 10^{+6}$	$2.123 \times 10^{+4}$
	500	$4.936 \times 10^{+5}$	$1.854 \times 10^{+4}$
0.06	425	$3.211 \times 10^{+6}$	$5.478 \times 10^{+4}$
	450	$2.155 \times 10^{+6}$	$4.863 \times 10^{+4}$
	475	$5.596 \times 10^{+5}$	$2.361 \times 10^{+4}$
	500	$3.952 \times 10^{+5}$	$2.195 \times 10^{+4}$
0.09	425	$4.769 \times 10^{+6}$	$8.179 \times 10^{+4}$
	450	$2.561 \times 10^{+6}$	$7.197 \times 10^{+4}$
	475	$7.316 \times 10^{+5}$	$4.872 \times 10^{+4}$
	500	$3.046 \times 10^{+5}$	$3.057 \times 10^{+4}$

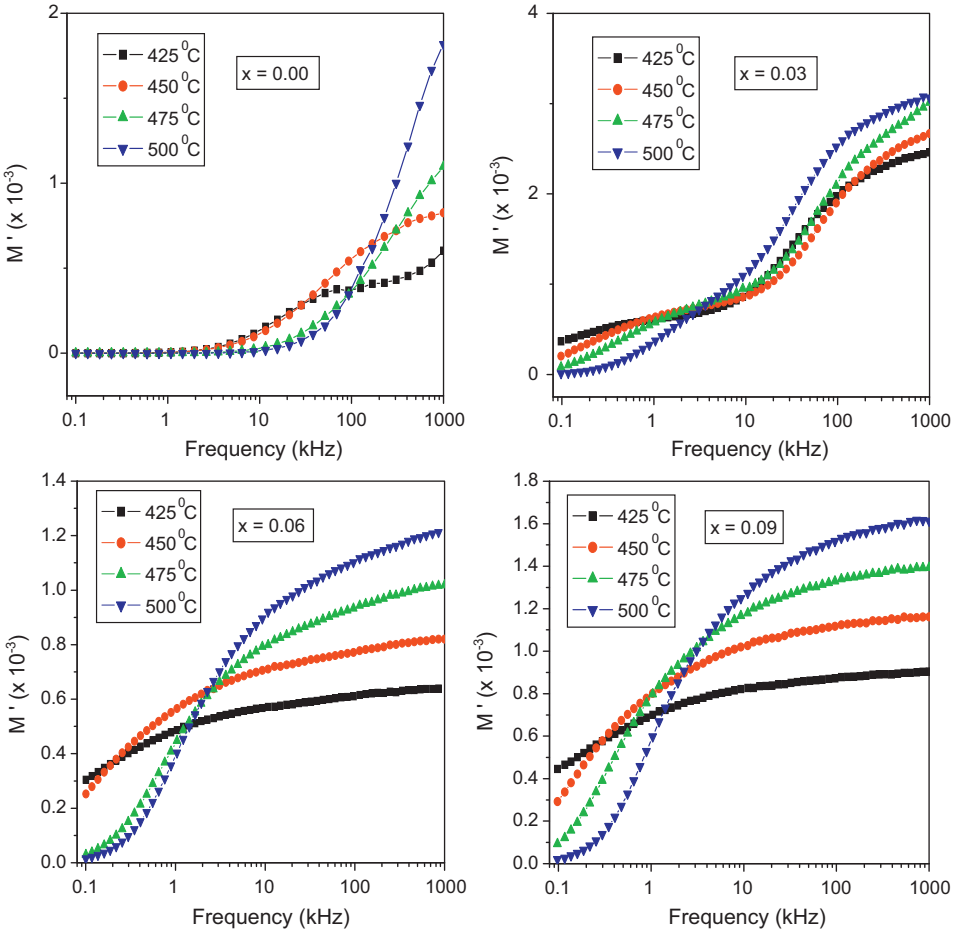

Fig. 4. Frequency–temperature dependence of M' of $Pb_{1-x}Sm_x(Zr_{0.55}Ti_{0.45})_{1-x/4}O_3$ with $x = 0.00$, 0.03, 0.06 and 0.09.

ture to compensate lead loss during the high temperature calcination and sintering. The oxides were mixed thoroughly in an alcohol medium and then calcined at an optimized temperature of 1100 °C for 10 h. Using polyvinyl alcohol (PVA), the calcined powders were cold pressed into cylindrical pellets of 10 mm diameter and 2.2 mm thickness at a pressure of 4×10^6 N/m^2 using a hydraulic press. PVA was used as binder to reduce the brittleness of the pellet, which burnt out during high temperature sintering. The pellets were, then, sintered at an optimized temperature of 1200 °C for 10 h so as to get nearly 97% of theoretical density.

For electrical measurements, flat surfaces of the pellets were polished and electroded with high purity air-drying silver paint. After electroding, the pellets were dried at 150 °C for 4 h to remove moisture. Using phase sensitive multimeter (PSM N4L; Model 1735), a number of electrical data were recorded at different temperatures and frequencies through which various electrical parameters were calculated.

3. Results and discussion

Microstructural and electrical properties of the polycrystalline PSZT ceramics were analyzed using complex impedance spectroscopy (CIS) technique [40]. It is a non-destructive experimental technique that helps in the measurement of real and imaginary components of the complex electric parameters. It provides nearly true picture of material properties. It analyzes the ac response of a system to a sinusoidal perturbation and helps in the calculation of impedance in terms of frequency. The frequency dependent electric parameters such as, complex impedance (Z^*), complex modulus (M^*), complex dielectric constant (ε^*) and tangent loss ($\tan\delta$) are related as; $Z^* = Z' - jZ''$, $M^* = (1/\varepsilon^*(\omega)) = M' + jM''$, $\varepsilon^* = \varepsilon' - j\varepsilon''$ and $\tan\delta = \varepsilon''/\varepsilon'$. Where ($Z'$, M', ε') and (Z'', M'', ε'') are the real and imaginary components of impedance, modulus and permittivity respectively, and $j = \sqrt{-1}$ the imaginary factor.

In CIS-technique, the experimental data are usually analyzed and interpreted with the help of equivalent circuit model representing the realistic material properties. These properties are determined by a series combination of grain and grain boundary, each represented by a parallel RC element. Its simplest appropriate equivalent circuit is a series array of two parallel RC elements.

To get maximum possible information about the electrical properties of materials, CIS-technique involves four fundamental formalisms: impedance formalism, admittance formalism, permittivity formalism and modulus formalism. Each of them provides a wide scope of graphical analysis concerning to these electrical properties. Though, Hodge et al. [41] has stressed that the combined analysis of complex impedance and complex modulus formalisms is advantageous in the study of solid electrolytes. Here, a parallel RC element gives rise a semicircle in the complex plane (Z' vs. Z'' and M' vs. M'') or a Debye peak in the spectroscopic plots of the imaginary component (Z'', M'' vs. $\log f$).

3.1. Complex impedance analysis of PSZT

The real part of impedance (Z') of the PSZT compounds under consideration exhibits a low frequency dispersion (not shown) due to polarization. At higher frequencies, it becomes almost independent of both the frequency and the temperature. The same variation has been found in case of imaginary part of impedance (Z'') of the PSZT compounds with frequency at lower temperatures. These support the increase in ac conductivity with temperature. The initial decrease in Z' with frequency may be due to a slow dynamic relax-

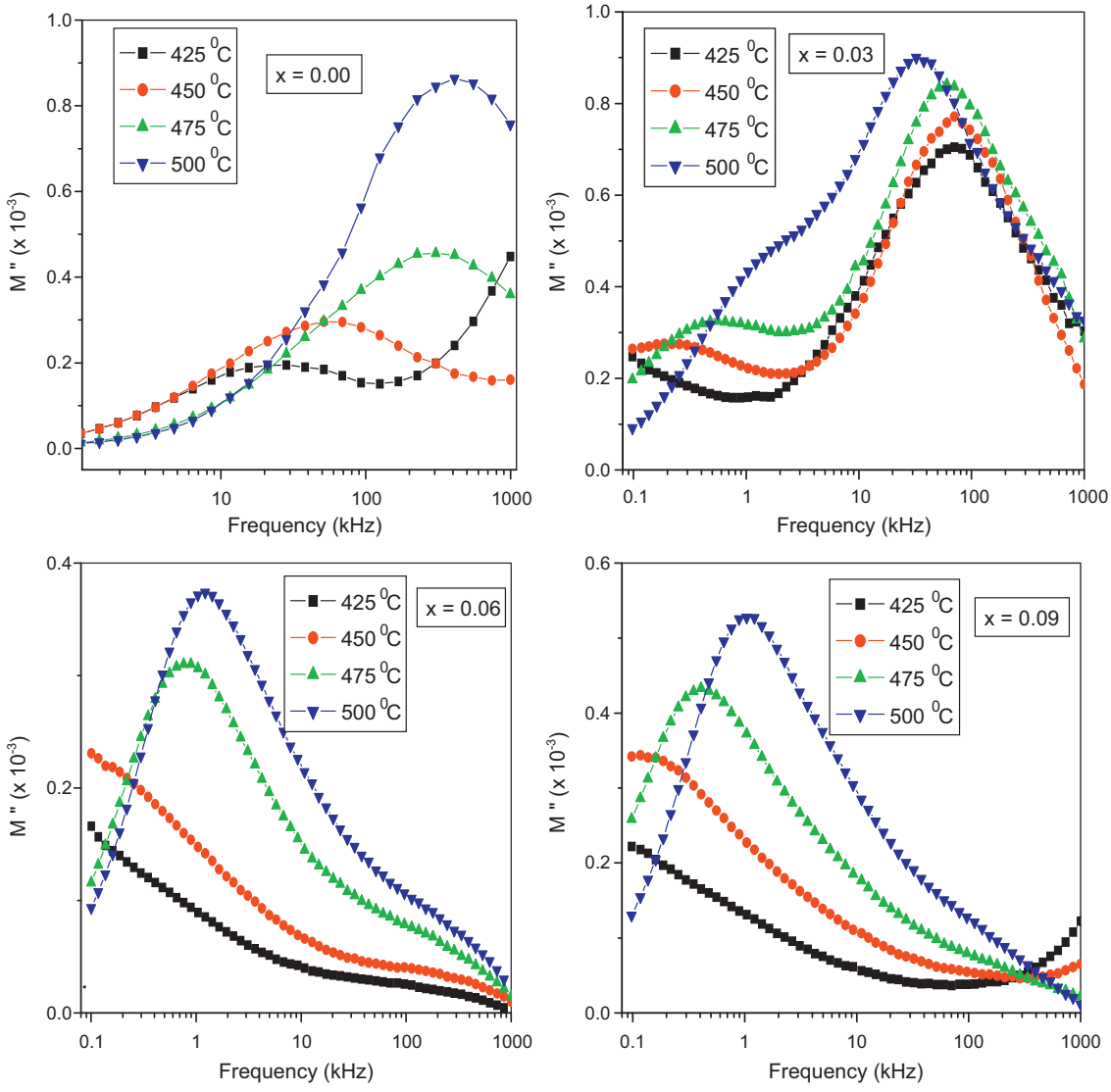

Fig. 5. Frequency–temperature dependence of M'' of $Pb_{1-x}Sm_x(Zr_{0.55}Ti_{0.45})_{1-x/4}O_3$ with $x = 0.00$, 0.03, 0.06 and 0.09.

ation process in the materials probably due to space charges that releases at higher frequencies [42–46].

Fig. 1 shows the variation of imaginary part of impedance (Z'') of the PSZT compounds with frequency at higher temperatures that exhibit some peaks. These peaks shift towards higher frequencies on increasing temperature in a broadening manner with the decrease in peak height. It indicates a thermally activated dielectric relaxation process in the materials and shows the reduction in the bulk resistance with temperature. But these peaks have not been found at low temperatures (not shown) which may be due to the weak current dissipation in the material or may be beyond the frequency of measurement. A significant broadening of the peaks with increase in temperature suggests the presence of temperature dependent relaxation process in the materials. The asymmetric broadening of peaks has also been observed which suggests the presence of some electrical processes in the materials with spread of relaxation time. These dispersion curves appear to merge at high frequency. This behavior is again due to the presence of space charge polarization at lower frequencies and its elimination at higher frequencies [47,48]. Z'' is also found to depend on samarium substitution to PZT. At higher temperatures, the peak height representing the relaxation shows an increasing trend with the increase in Sm-content from 0% to 9%.

The complex impedance spectrum (Z' vs. Z'' called Nyquist plot) of $Pb_{1-x}Sm_x(Zr_{0.55}Ti_{0.45})_{1-x/4}O_3$ compounds at selected temperatures is shown in Fig. 2, which exhibits single semicircular arc (or its tendency) at a particular temperature. The appearance of full, partial or no semicircle depends upon the strength of relaxation and the available frequency range [49–51]. Though, these semicircles are depressed semicircles with centers lying below the real Z' axis (not shown). It confirms the presence of non-Debye type of relaxation in the materials. The absence of second semicircle in the complex impedance plots suggests the dominance of bulk contributions in the PSZT compounds. Using the computer program 'ZSimpWin', the fitted complex impedance plots of the samples at 500 °C along with the equivalent circuit model are shown in Fig. 3. In order to represent the non-ideal Debye type behavior, a constant phase element (CPE) is introduced with the resistors and capacitors. It has an impedance given by Abram et al. [52], $Z_{CPE} = [A_0(j\omega)^n]^{-1}$, where $A_0 = A/\cos(n\pi/2)$ and $j = \sqrt{-1}$. 'A' and 'n' are frequency independent parameters of Jonscher's power law [47,53]. The value of n lies between 0 and 1 ($n = 1$ for an ideal capacitor and $n = 0$ for ideal resistor). Fitting parameters with equivalent circuit [(CR)(CQR)] of PSZT are given in Table 1. The values of bulk resistance (R_b) and grain boundary resistance (R_{gb}) obtained from the intercept of semicircular arcs on the real axis (Z') at different temperatures are

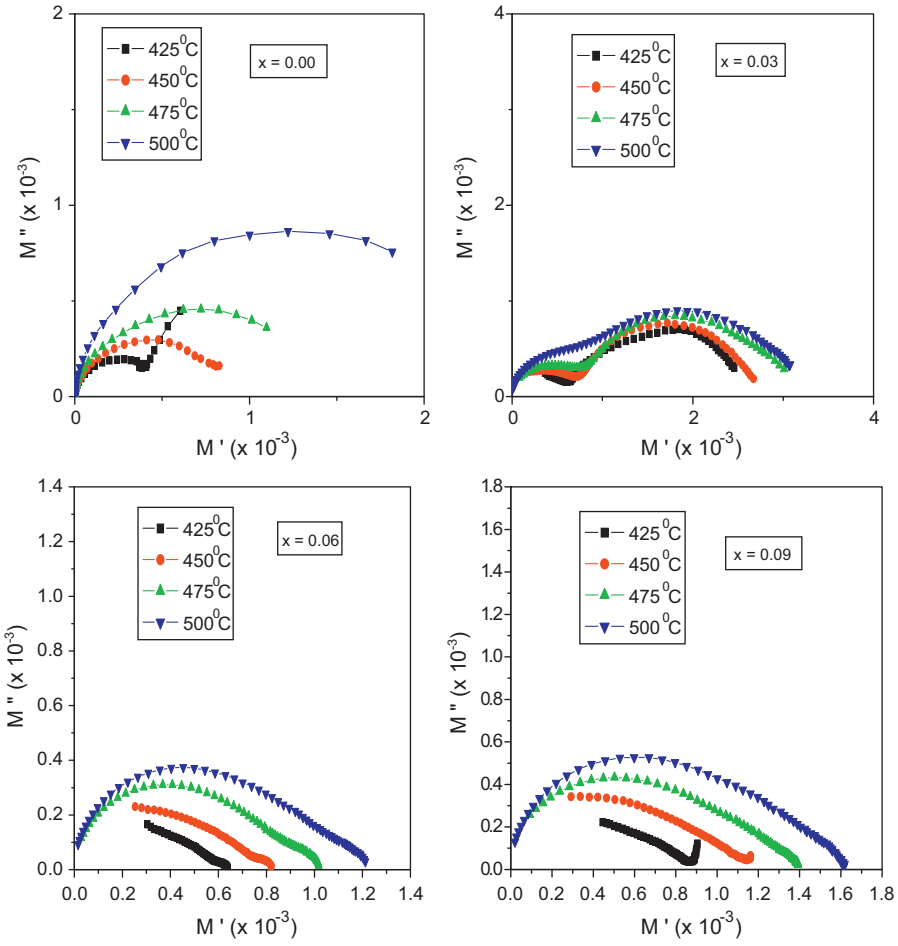

Fig. 6. Variation of M' with M'' of $Pb_{1-x}Sm_x(Zr_{0.55}Ti_{0.45})_{1-x/4}O_3$ at selected temperatures with $x = 0.00$, 0.03, 0.06 and 0.09.

given in Table 2. Here, it is observed that the grain and grain boundary resistances of each of the PSZT composition exhibit decreasing trends with the increase in temperature. It indicates that the conductivity increases with increase in temperature supporting the typical negative temperature coefficient of resistance (i.e., NTCR) behavior of the materials usually shown by semiconductors.

3.2. Complex modulus analysis of PSZT

Frequency–temperature dependence of the real part of electric modulus (M') of PSZT compounds is shown in Fig. 4. The value of M' is found to be very low (nearly zero) at low frequencies and it increases with the increase in frequency. This continuous dispersion on increasing frequency may be contributed to the conduction phenomena due to short range mobility of charge carriers. It is possibly related to the lack of restoring force governing the mobility of the charge carriers under the action of an induced electric field [54]. M' is also found to increase with the increase in temperature which attributes a temperature dependent relaxation process in the materials. It is also found that the dispersion region shifts towards higher frequency side which suggests the long-range mobility of charge carriers. The plateau region or its tendency observed at higher frequencies suggests about the frequency invariant (dc conductivity) electrical properties of the materials. The value of M' is found to be dependent on the samarium substitution to PZT. It exhibits a small value in case of unmodified PZT. With the increase in Sm^{3+} content of PSZT, it exhibits a rise when $x = 0.03$, a fall when $x = 0.06$ and again a small rise when $x = 0.09$.

The variation of imaginary part of electric modulus (M'') of $Pb_{1-x}Sm_x(Zr_{0.55}Ti_{0.45})_{1-x/4}O_3$ ($x = 0.00$, 0.03, 0.06 and 0.09) with frequency at selected temperatures is shown in Fig. 5. It exhibits peak (or its tendency) in the low as well as high frequency side. The low frequency side peak indicates that the ions can move over long distances whereas high frequency side peak suggests the confinement of ions in their potential well. These two peaks indicate the transition from long-range to short-range mobility on increasing frequency [55]. The observed asymmetry in peak broadening indicates the spread of relaxation time with different time constant which supports the non-Debye type of relaxation in the materials. It is also observed that the peaks are shifting towards higher frequency side with the increase in temperature. It indicates thermally activated behavior of relaxation time. This type of effect has also been observed in the modulus spectra of real ionic conductors [56,57]. The low value of M'' observed at lower frequencies may occur due to the absence of electrode polarization phenomena. The value of M'' corresponding to the peaks depends upon Sm^{3+} concentration in PSZT. It exhibits a small value in case of unmodified PZT. With the increase in Sm-content, it shows a small rise when $x = 0.03$, a considerable fall when $x = 0.06$ and again a small rise when $x = 0.09$.

The temperature dependence of the complex modulus spectrum (M' vs. M'') of PSZT ceramics is shown in Fig. 6. The appearance of an arc in the spectrum at a particular temperature confirms the single phase character of the materials. At higher temperatures, these arcs are not exact semicircle(s). They are in the form of two deformed semi-circles (or their tendency) with their centers lying below the real axis. This indicates spread of relaxation with different (mean)

time constant and hence again supports the non-Debye type of relaxation in the materials. The two semicircular arcs or their tendency in the complex modulus plots suggest the presence of both the grain and grain boundary contributions in the PSZT compounds. It is also observed that with the increase in temperature, intercept of the arcs on real M' axis shift towards the higher values of M' which indicates about the increase in capacitance. It supports the negative temperature coefficient of resistance (NTCR) type behavior of the materials since bulk capacitance (C_b) is inversely proportional to the bulk resistance (R_b). At higher temperatures and lower frequencies, tails are not fully evolved to its true shape which may be due to frequency and temperature limitations. The single semicircular arcs in Fig. 2 exhibit the dominant bulk (grain) contribution whereas the double semicircular arcs in Fig. 6 suggest the presence of both the bulk (grain) and grain boundary contributions. It is based on the fact that the impedance plot highlights the phenomenon with the largest resistance whereas modulus plot picks out those of the smallest capacitance. With the huge difference (orders of magnitude) between the resistive values of grains and grain boundaries, it is difficult to obtain two full semicircles for grains and grain boundary on the same scale in the impedance plot. Complex modulus analysis is suitable when materials have nearly similar resistance but different capacitance [58].

4. Conclusions

The PSZT ceramic samples with Zr/Ti ratio 55/45 and samarium content $x = 0.00$, 0.03, 0.06 and 0.09 were prepared by solid-state reaction technique at high temperature. The impedance and electric modulus properties of the materials have been investigated with the help of complex impedance spectroscopy (CIS) technique. Single arc with single/double semicircle(s) (or tendency) obtained at a particular temperature corresponding to a certain PSZT composition in both the complex impedance and modulus plots suggests the single phase character of the materials. It has been already reported elsewhere [39]. The impedance analysis has indicated the presence of mainly bulk (grain) contributions in the materials which is found to decrease with the increase in temperature. It shows that the PSZT compounds exhibit negative temperature coefficient of resistance (NTCR) type behavior usually found in semiconductors. The complex modulus plots have indicated the presence of grain boundary along with the bulk contributions in the materials. This complex modulus analysis has also supported the NTCR behavior of PSZT compounds as the capacitance of the materials increases with the increase in temperature. Also, the impedance as well as modulus analysis has confirmed the presence of non-Debye type of relaxation in the PSZT compounds.

Acknowledgement

One of the authors (NK) wishes to acknowledge the Council of Scientific and Industrial Research, New Delhi (India) for financial support.

References

[1] M.E. Lines, A.M. Glass, Principles and Applications of Ferroelectrics and Related Materials, Oxford University Press, Oxford, 1977.
[2] G. Shirane, K. Suzuki, J. Phys. Soc. Jpn. 7 (1952) 333–1333.
[3] B.V. Hiremath, A.I. Kingon, J.V. Biggers, J. Am. Ceram. Soc. 66 (1983) 790–793.
[4] T. Ohno, M. Takahashi, N. Tsubouchi, J. Jpn. Soc. Powder Powder Metall. 20 (1973) 154–160.
[5] S.S. Chandratreya, R.M. Fulrath, J.A. Pask, J. Am. Ceram. Soc. 64 (1981) 422–425.
[6] Q. Zhou, S. Lau, D. Wu, K.K. Shung, Prog. Mater. Sci. 56 (2011) 139–174.
[7] Y. Yang, B.S. Divsholi, C.K. Soh, Sensors 10 (2010) 5193–5208.
[8] B. Belgacem, F. Calame, P. Muralt, J. Electroceram. 19 (2007) 369–373.
[9] W. Liu, J.S. Ko, W. Zhu, Ferroelectrics 263 (2001) 19–25.
[10] Y.L. Wang, Z.M. Cheng, Y.R. Sun, X.H. Dai, Physica B+C 150 (1988) 168–174.
[11] M. Ozolinsh, K. Stock, R. Hibst, R. Steiner, IEEE J. Quantum Electron. 33 (1997) 1846–1849.
[12] J. Soman, C.B. O'Neal, IEEE Sens. J. 11 (2011) 78–85.
[13] B. Jaffe, W.R. Crook, H. Jaffe, Piezoelectric Ceramics, Academic Press, New York, 1971.
[14] W.L. Zhong, Y.G. Wang, P.L. Zhang, B.D. Qu, Phys. Rev. B 50 (1994) 698–703.
[15] R.S. Nasar, M. Cerqueira, E. Longo, J.A. Varela, A. Beltran, J. Eur. Ceram. Soc. 22 (2002) 209–218.
[16] S.A. Mabud, J. Appl. Crystallogr. 13 (1980) 211–216.
[17] A.P. Smyth, Dielectric Behavior and Structure, McGraw Hill Publishers, New York, 1955.
[18] G.H. Haertling, J. Am. Ceram. Soc. 82 (1999) 797–818.
[19] K. Ramam, A.J. Bell, C.R. Bowen, K. Chandramouli, J. Alloys Compd. 473 (2009) 330–335.
[20] R.A. Roca, E.R. Botero, F. Guerrero, J.D.S. Guerra, D. Garcia, J.A. Eiras, J. Appl. Phys. 105 (2009) 014110–14115.
[21] E.R. Camargo, E.R. Leite, E. Longo, J. Alloys Compd. 469 (2009) 523–528.
[22] W. Qiu, H.H. Hng, Mater. Chem. Phys. 75 (2002) 151–156.
[23] K. Ramam, M. Lopez, J. Alloys Compd. 466 (2008) 398–403.
[24] S. Dutta, R.N.P. Choudhary, P.K. Sinha, J. Alloys Compd. 430 (2007) 344–349.
[25] S.N. Kallaev, Z.M. Omarov, R.G. Mitarov, A.R. Bilalov, K. Bormanis, S.A. Sadykov, J. Exp. Theor. Phys. 111 (2010) 3421–3426.
[26] S.R. Shannigrahi, R.N.P. Choudhary, J. Eur. Ceram. Soc. 24 (2004) 163–170.
[27] R. Khazanchi, S. Sharma, T.C. Goel, J. Electroceram. 14 (2005) 113–118.
[28] S.R. Shannigrahi, R.N.P. Choudhary, Br. Ceram. Trans. 101 (2002) 25–29.
[29] R. Rai, S. Mishra, N.K. Singh, J. Alloys Compd. 487 (2009) 494–498.
[30] R. Rai, S. Sharma, R.N.P. Choudhary, Solid State Commun. 133 (2005) 635–639.
[31] S.Q. Zhang, L.D. Wang, W.L. Li, N. Li, W.D. Fei, J. Alloys Compd. 509 (2011) 2976–2980.
[32] U. Chon, K. Bum, H.M. Jang, G.C. Yi, Appl. Phys. Lett. 79 (2001) 3137–3139.
[33] S.K. Pandey, S. Kumar, S.N. Chatterjee, U. Kumar, C. Prakash, R. Chatterjee, T.C. Goel, Physica B 388 (2007) 404–411.
[34] D.K. Mahato, R.K. Choudhary, S.C. Srivastava, J. Appl. Sci. 6 (2006) 716–720.
[35] C. Prakash, O.P. Thakur, Mater. Lett. 57 (2003) 2310–2314.
[36] C. Pramila, T.C. Goel, P.K.C. Pillai, Mater. Sci. Eng. B 26 (1994) 25–28.
[37] S.K. Pandey, O.P. Thakur, D.K. Bhattacharya, C. Prakash, R. Chatterjee, J. Alloys Compd. 468 (2009) 356–359.
[38] A.K. Tripathi, T.C. Goel, C. Prakash, Mater. Sci. Eng. B 96 (2002) 19–23.
[39] R. Ranjan, R. Kumar, B. Behera, R.N.P. Choudhary, Mater. Chem. Phys. 115 (2009) 473–477.
[40] J.R. Macdonald, Impedance Spectroscopy, John Wiley and Sons, 1987.
[41] I.M. Hodge, M.D. Ingram, A.R. West, J. Electroanal. Chem. 74 (1976) 125–143.
[42] J. Suchanicz, Mater. Sci. Eng. B 55 (1998) 114–118.
[43] J. Plocharski, W. Wieczoreck, Solid State Ionics 28–30 (1988) 979–982.
[44] C.K. Suman, K. Prasad, R.N.P. Choudhary, Bull. Mater. Sci. 27 (2004) 547–553.
[45] K. Srinivas, P. Sarah, S.V. Suryanarayana, Bull. Mater. Sci. 26 (2003) 247–253.
[46] M.R. Rangaraju, R.N.P. Choudhary, J. Mater. Sci. 39 (2004) 1765–1771.
[47] A.K. Jonscher, Nature 267 (1977) 673–679.
[48] K.S. Rao, D.M. Prasad, P.M. Krishnal, J.H. Lee, Eur. Phys. J. Appl. Phys. 41 (2008) 229–236.
[49] D.C. Sinclair, A.R. West, J. Mater. Sci. 29 (1994) 6061–6068.
[50] M.A.L. Nobre, S. Lanfredi, J. Phys. Chem. Solids 64 (2003) 2457–2464.
[51] R. Gerhardt, J. Phys. Chem. Solids 55 (1994) 1491–1506.
[52] E.J. Abram, D.C. Sinclair, A.R. West, J. Electroceram. 10 (2003) 165–178.
[53] J.B. Jorcin, M.E. Orazem, N. Pebere, B. Tribollet, Electrochim. Acta 51 (2006) 1473–2179.
[54] P.B. Macedo, C.T. Moynihan, R. Bose, Phys. Chem. Glasses 13 (1972) 171–179.
[55] F. Borsa, D.R. Torgeson, S.W. Martin, H.K. Patel, Phys. Rev. B 46 (1992) 795–800.
[56] V. Provenzano, L.P. Boesch, V. Volterra, C.T. Moynihan, P.B. Macedo, J. Am. Ceram. Soc. 55 (1972) 492–496.
[57] H. Jain, C.H. Hsieh, J. Non-Cryst. Solids 172–174 (1994) 1408–1412.
[58] P. Victor, S. Bhattacharyya, S.B. Krupanidhi, J. Appl. Phys. 94 (2003) 5135–5142.